3606–3613 *Nucleic Acids Research, 2005, Vol. 33, No. 11*
doi:10.1093/nar/gki677

A T-stem slip in human mitochondrial tRNA^{Leu}(CUN) governs its charging capacity

Rui Hao[1], Ming-Wei Zhao[1], Zhan-Xi Hao[1], Yong-Neng Yao and En-Duo Wang[1,*]

State Key Laboratory of Molecular Biology and [1]Graduate School of the Chinese Academy of Sciences, Institute of Biochemistry and Cell Biology, Shanghai Institutes for Biological Sciences, The Chinese Academy of Sciences, 320 Yue Yang Road, Shanghai 200031, People's Republic of China

Received April 7, 2005; Revised and Accepted June 9, 2005

ABSTRACT

The human mitochondrial tRNA^{Leu}(CUN) [hmtRNA^{Leu}(CUN)] corresponds to the most abundant codon for leucine in human mitochondrial protein genes. Here, *in vitro* studies reveal that the U48C substitution in hmtRNA^{Leu}(CUN), which corresponds to the pathological T12311C gene mutation, improved the aminoacylation efficiency of hmtRNA^{Leu}(CUN). Enzymatic probing suggested a more flexible secondary structure in the wild-type hmtRNA^{Leu}(CUN) transcript compared with the U48C mutant. Structural analysis revealed that the flexibility of hmtRNA^{Leu}(CUN) facilitates a T-stem slip resulting in two potential tertiary structures. Several rationally designed tRNA^{Leu}(CUN) mutants were generated to examine the structural and functional consequences of the T-stem slip. Examination of these hmtRNA^{Leu}(CUN) mutants indicated that the T-stem slip governs tRNA accepting activity. These results suggest a novel, self-regulation mechanism of tRNA structure and function.

INTRODUCTION

In protein biosynthesis, transfer RNAs (tRNAs) play a central role in gene expression as adaptor molecules of the codons in mRNA and amino acids (1). The human mitochondrial translation machinery is dependent on 22 tRNAs, one for each of 18 amino acids and two for Leu and Ser with different anticodons (2). All of these tRNAs are encoded by the mitochondrial genome. The primary and secondary structures of human mitochondrial tRNAs (hmtRNAs) differ significantly from those of canonical bacterial and cytoplasmic tRNAs, and tRNAs in human mitochondria are less thermodynamically stable because they generally contain higher numbers of mismatched and AU base pairs (3). Therefore, while hmtRNAs should adopt an L-shape tertiary structure of canonical tRNA in order to function in ribosomal protein synthesis, their folded structures may be constructed with different sets of intramolecular contacts that are mostly unknown.

In the past 15 years, a number of point mutations in hmtRNA genes have been found to be correlated with a variety of multi-system diseases (4,5). Although the molecular mechanisms of these mitochondrial DNA-mediated diseases remain unclear, accumulating evidence has shown that severe structural and functional defects of hmtRNAs are caused by the pathogenic mutations (6–8). Systematic investigation of the structure and function of hmtRNAs can, therefore, provide valuable information about related diseases and potentially facilitate development of diagnostic tools and therapies for these diseases.

Among the 22 hmtRNAs, hmtRNA^{Leu}(CUN) corresponds to the most frequently used codon (14.9%) (9). Even a slight impairment of the function of hmtRNA^{Leu}(CUN) can lead to significant deficiencies in mitochondrial protein synthesis. Although tRNA^{Leu}(CUN) is one of the few mitochondrial tRNAs that possesses all of the structural features for a classical cloverleaf structure and 3D folding (3), little information is available about the structure and function of hmtRNA^{Leu}(CUN).

Among the five known pathogenic mutations in the hmtRNA^{Leu}(CUN) gene (see http://www.mitomap.org) is the T12311C mutation (10) that sparks our interest. This mutation resides at residue 48, which is the connector between the variable loop and the T-stem in the tRNA secondary structure (Figure 1A). It is hypothesized that the tertiary interaction between nt 15 and 48 plays an important role in the tRNA 3D structure; replacement of either of these 2 nt affects tRNA conformation (11). In this *in vitro* study, a U48C substitution was introduced in the hmtRNA^{Leu}(CUN) gene, mimicking the T12311C mutation, in order to examine changes in structure and aminoacylation of hmtRNA^{Leu}(CUN). Surprisingly, the tRNA accepting capacity and structural stability were increased by this substitution. Secondary structure analysis of hmtRNA^{Leu}(CUN) suggested two kinds of pairing alignments

*To whom correspondence should be addressed. Tel: +86 21 54921241; Fax: +86 21 54921011; Email: edwang@sibs.ac.cn

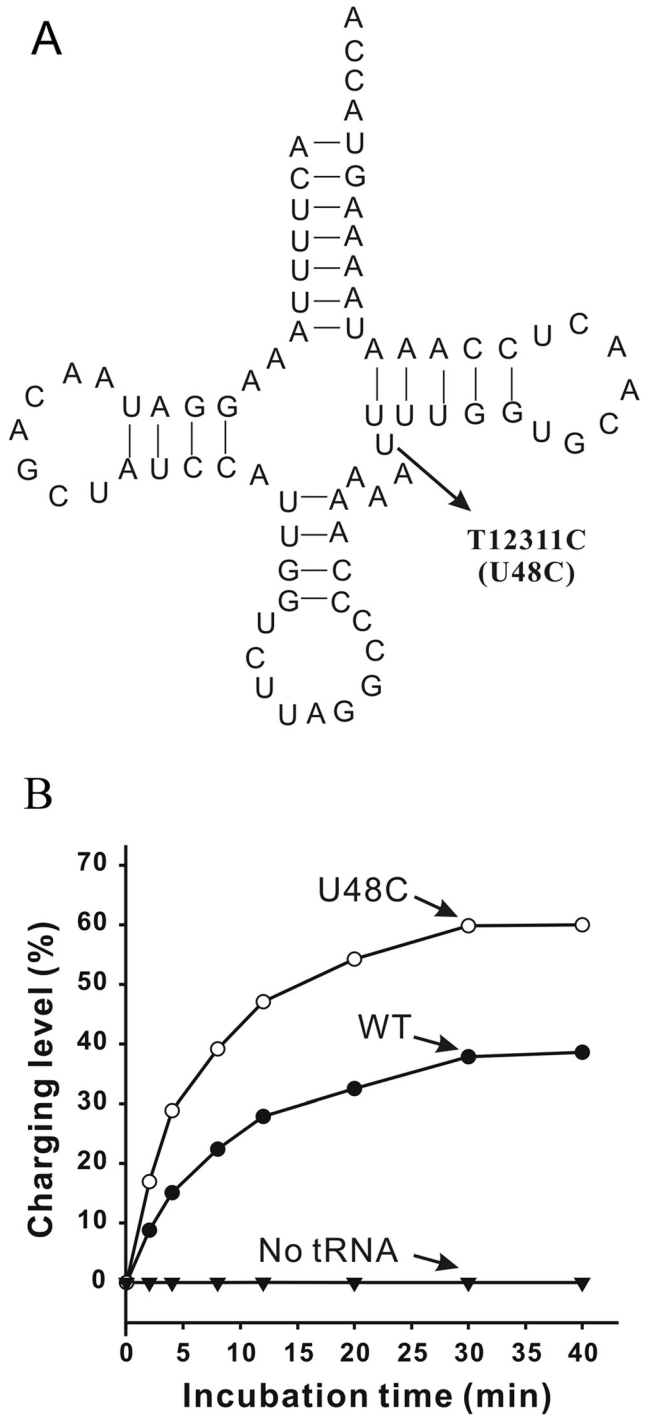

Figure 1. The effect of pathogenic T12311C (U48C) mutation on the aminoacylation hmtRNA^{Leu}(CUN). (**A**) Theoretical cloverleaf structure of tRNA^{Leu}(CUN) as deduced from the DNA sequence. The pathogenic point mutation T12311C (U48C) is indicated with arrow. (**B**) Aminoacylation of WT hmtRNA^{Leu}(CUN) and U48C mutant transcripts.

in the T-stem that could be formed by a 1 nt slip. We subsequently constructed a series of hmtRNA^{Leu}(CUN) mutants to mimic the different types of tertiary structures resulting from the T-stem slip and studied their structures and aminoacylation capacities. Here, we analyze the structural basis of T-stem slip and the resulting tertiary structures that provide evidence for a novel, self-regulating acceptance mechanism of hmtRNA^{Leu}(CUN).

MATERIALS AND METHODS

Enzyme purification and tRNA preparation

All chemicals were purchased from Sigma–Aldrich Inc. (USA), except otherwise noted.

T7 RNA polymerase and human mitochondrial leucyl-tRNA synthetase (hmLeuRS) were purified from *Escherichia coli* overproducing strains as described previously in our laboratory (12,13). *In vitro* transcription of mitochondrial tRNA and subsequent refolding of tRNA were performed as described previously (14). The tRNA concentration was determined by UV absorbance at 260 nm and the extinction coefficient was calculated from the sequence of each tRNA (15).

Assaying aminoacylation of tRNA transcript using [^{14}C]leucine

Accepting activity of the tRNA transcript and the time course of tRNA aminoacylation were assessed as described previously (14). The optimized reaction mixture contained 50 mM HEPES, pH 7.6, 25 mM KCl, 10 mM $MgCl_2$, 2.5 mM ATP, 1 mM spermidine, 100 μg/ml BSA, 20 μM L-[^{14}C]leucine, 0.5 μM hmLeuRS and 1.5 μM hmtRNA^{Leu}(CUN) transcript. The aminoacylation plateau was determined during a 40 min incubation time. The charging level of each tRNA transcript was calculated as the percentage of aminoacylated tRNA versus the total amount of specific tRNA per experiment. The apparent kinetic parameters, k_{cat} and K_M, of hmLeuRS for hmtRNA^{Leu}(CUN) and its mutants were derived from Lineweaver-Burk plots on experiments performed with 1–50 μM tRNA and 0.15 μM hmLeuRS. Displayed data were the averages of three independent experiments.

Secondary structure prediction of tRNA

MFOLD 3.1 program (http://www.bioinfo.rpi.edu/~zukerm/) was used to analyze the secondary structure of tRNA (16). Parameters were used in default settings, except for percent suboptimality, which was set as 50%. Only cloverleaf-like structures were considered.

Nuclease mapping of tRNA structure in solution

tRNA transcripts were 5′-end-labeled with ^{32}P by the reaction with T4 polynucleotide kinase (New England Biolabs, Canada) and [γ-^{32}P]ATP as described previously (17). The purified ^{32}P-labeled transcripts were denatured by heating to 60°C in the absence of Mg^{2+} and then cooled slowly in the presence of 10 mM $MgCl_2$ (18). ^{32}P-labeled tRNAs were digested with various nucleases at 25°C for 10 min in 20 μl of 40 mM Tris–HCl, pH 7.5, 10 mM $MgCl_2$ and 40 mM NaCl. For digestion with nuclease S1 (Amersham Pharmacia, UK), 1 mM $ZnCl_2$ was added. The digestion reaction mixtures contained 10 000 c.p.m. ^{32}P-labeled tRNA, 4 μg non-labeled carrier tRNA and 0.1 or 2.0 U RNase T1 (Amersham, USA), 0.035 or 0.1 U RNase V1 (Ambion, USA) and 50 or 150 U nuclease S1, respectively. Reactions were stopped by adding 8 μg of carrier tRNA, chilling on ice and phenol extraction. The digested products were recovered by ethanol precipitation.

The pellets were resuspened in 10 µl of dye mix solution [0.0125% xylene cyanol and 0.0125% bromphenol blue in 50% formamide]. Samples were run on a 21 cm (width) × 50 cm (height) × 0.4 mm (diameter) 12% polyacrylamide gel containing 8 M urea buffered with 1× TBE, pH 8.3). Alkaline ladders and G-ladders were obtained as described previously (19).

RESULTS

Aminoacylation capacity of tRNA^{Leu}(CUN) was increased by the pathogenic T12311C (U48C) mutation

In the hmtRNA^{Leu}(CUN) gene, the pathogenic T12311C mutation changes the U to C at position 48, which is the connecting base between the variable loop and the T-stem (Figure 1A). We constructed the wild-type (WT) hmtRNA^{Leu}(CUN) and the U48C mutant *in vitro* and tested their aminoacylation efficiency by the cognate hmLeuRS.

Interestingly, the accepting activity of the mutant tRNA with the U48C substitution was increased compared with the WT (Figure 1B). Under optimal conditions, 40% of the WT transcript was aminoacylated (compared with the calculated theoretical accepting activity of the transcript, see Materials and Methods), while the accepting activity of the U48C mutant was >60%. Kinetic aminoacylation assays were further performed with 1–50 µM tRNA and 0.15 µM hmLeuRS. The kinetic parameters k_{cat} and K_M were determined for both the mutant and WT transcripts. Establishment of these parameters enables a valuable comparison of aminoacylation efficiency (k_{cat}/K_M). The increase of charging capacity was further evidenced by the finding that the U48C mutant was leucylated with a 1.31-fold higher efficiency than the WT hmtRNA^{Leu}(CUN) (Table 1).

Because magnesium ions may affect tRNA folding, we assayed the denaturing/renaturing processes with several concentrations of magnesium (from 3 to 20 mM) for each transcript. Similar aminoacylation levels of WT and mutant tRNA were obtained under all of these conditions (data not shown), indicating that magnesium ion concentration had little effect on hmtRNA^{Leu}(CUN) folding.

Structure analysis of hmtRNA^{Leu}(CUN)

In order to understand the relatively lower aminoacylation efficiency of the WT transcript, we examined the secondary structure of hmtRNA^{Leu}(CUN) using the MFOLD program (16) and enzymatic probing (20).

Secondary structure calculation revealed that there were two types of T-stem base pair alignments in the hmtRNA^{Leu}(CUN) transcript. In one alignment (Ta alignment), the U48 was located between the T-stem and variable loop as an unpaired connector and the T-loop contained 7 nt. In the other alignment (Tb alignment), the U48 paired with A65 in the T-stem and the enlarged T-loop contained 8 nt. Thus, the Ta alignment could become the Tb alignment by a 1 nt slip, which formed a base pair between 48 and 65 bases (Figure 2A). Because the U48C substitution decreased the tendency to form a base pair between C48 and A65, thus prohibiting the T-stem slip, most of the U48C transcript was stabilized in Ta alignment.

Considering the limitations of the MFOLD prediction (e.g. its ignorance of RNA 3D structure), we carried out an enzymatic probing experiment to detect the solution structure of the WT and mutant transcripts. The results of the enzymatic probing of hmtRNA^{Leu}(CUN) were in agreement with the MFOLD prediction described above. Nuclease S1 and RNase T1 (guanine specific) were used to probe the unpaired nucleotides, and RNase V1 was used to monitor base-paired or stacked nucleotides. The 5′-end-labeled cleaved fragments were separated by PAGE/urea. As the nonspecific cleavage of the transcripts at certain weak points could affect the results, each of these enzymes was used with different concentrations. Only dose-dependent enzymatic cleavages were considered. The autoradiograms are presented in Figure 3A and results of enzymatic mapping are summarized in Figure 3B.

Most of the nucleotides within the theoretical stem regions of the WT hmtRNA^{Leu}(CUN) were cleaved by RNase V1 and most of those within the canonical loop regions were recognized by nuclease S1. The hmtRNA^{Leu}(CUN) transcript appears to fold into the classical cloverleaf structure despite the absence of post-transcriptional modification. The general cleavage patterns of the WT and U48C mutant were similar to each other except for some minor differences in their T-loops. The WT transcript was cleaved by RNase T1 at G53, which is thought to be paired with C61 in the Ta alignment. This indicated that at least some proportion of the WT transcript existed in the Tb alignment, in which G53 remained unpaired in the T-loop. The cleavage at G53 by RNase T1 was dose-dependent in three separate experiments (data not shown), suggesting that the result is not related to the quality of the gel. However, in the case of U48C mutant, no corresponding cleavage was observed. The differences in the enzymatic digestion patterns

Table 1. Apparent kinetic parameters of *in vitro* aminoacylation of WT and mutant hmtRNA^{Leu}(CUN) transcripts by human mitochondrial leucyl-tRNA synthetase

hmtRNA^{Leu}(CUN) transcripts	$k_{cat}(10^{-3}\ s^{-1})$	$K_M(\mu M)$	$k_{cat}/K_M(10^{-3}\ s^{-1}\ \mu M^{-1})$	Relative k_{cat}/K_M
Wild type	52.4 ± 1.8	23.9 ± 3.9	2.19	1
U48C	112.3 ± 1.0	39.1 ± 5.7	2.87	1.31
U48G	115.5 ± 3.2	36.3 ± 6.9	3.18	1.45
U48A	110.3 ± 2.2	37.2 ± 5.3	2.96	1.35
Δ48	123.1 ± 4.7	34.9 ± 2.6	3.53	1.61
G52A/C62G	53.8 ± 3.2	11.5 ± 2.5	4.68	2.13
U51A/A63U	56.2 ± 4.9	8.8 ± 1.6	6.39	2.91
U51G	<0.0001	Nd	–	–
U48C/+G54	<0.0001	Nd	–	–

Aminoacylation reactions were as described in Materials and Methods. Data presented here were the average of three independent experiments.
Nd, not determined.

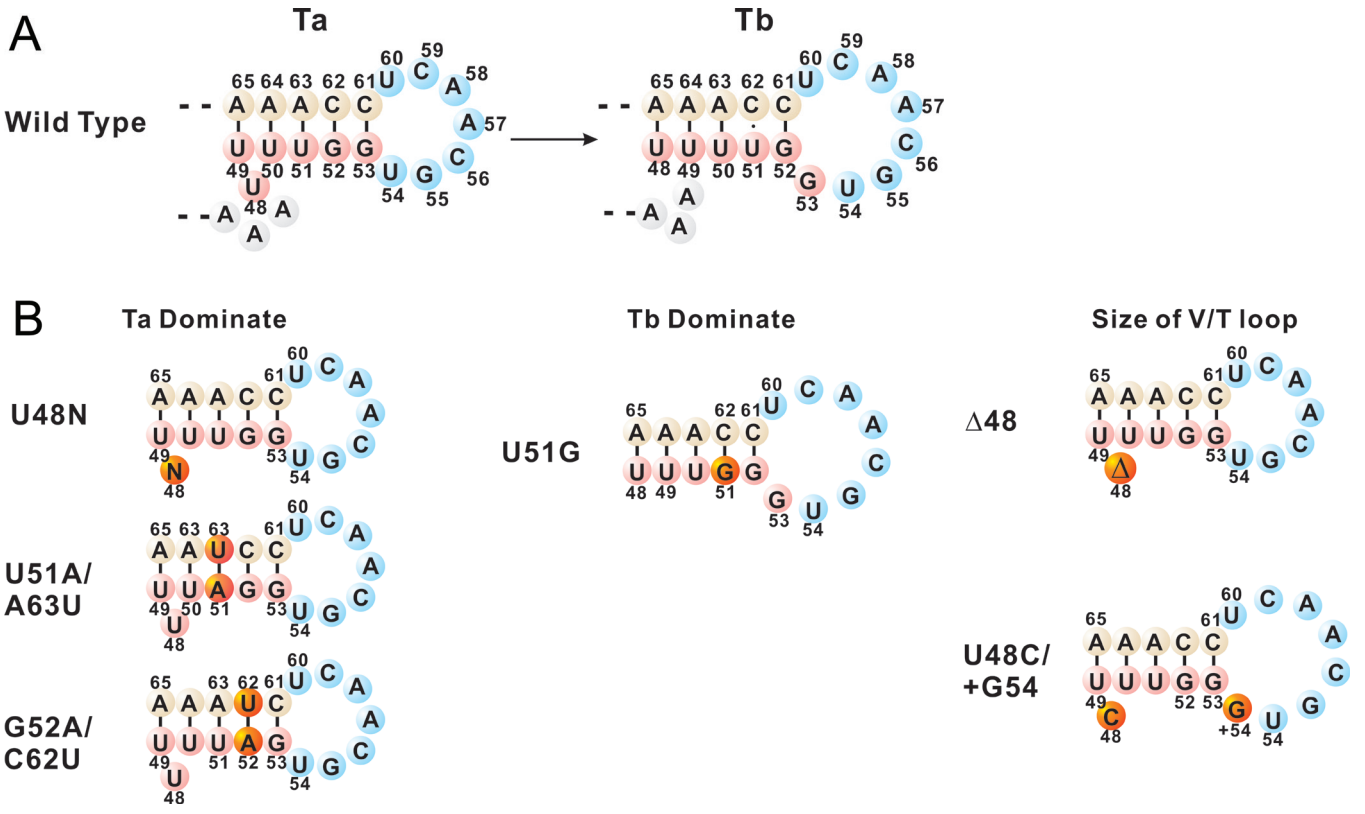

Figure 2. Predicated T-stem secondary structures of WT hmtRNA^{Leu}(CUN) and the designed variants. Numbering of the nucleotides is according to Sprinzl *et al.* (39). (**A**) Two alternative T-stem alignments in WT hmtRNA^{Leu}(CUN) transcript. U48 at the variable loop of Ta alignment slips to T-stem and forms a new U48:A65 base pair in Tb alignment with 8 nt T-loop; (**B**) various hmtRNA^{Leu}(CUN) constructs with designed T-stem. The U48N (N = A, G, C), G52A/C62U and U51A/A63U mutants were dominated in the Ta alignment; the U51G mutation was dominated in the Tb alignment; the Δ48 and U48C/+G54 mutants were designed to mimic the effect of T-stem slip on V-loop and T-loop, respectively.

of the WT and U48C mutant are summarized in Figure 3B. It appears that the fragment indicated with a pentacle in Figure 3B was due to the U48 shift in the T-stem.

Manipulation of the T-stem slip of hmtRNA^{Leu}(CUN)

To investigate the effect of the different T-stem base pair alignments on the structure and aminoacylation of hmtRNA^{Leu}(CUN), we constructed mutants of hmtRNA^{Leu}(CUN) that would stabilize in either the Ta or Tb alignment depending on the T-stem structure (Figure 2B). Similar to U48C mutant, U48A and U48G mutants were created to restrain the T-stem slip by prohibiting the base pairing between 48 and 65 residues. These two mutants would theoretically stabilize in the Ta alignment. Two double mutations, U51A/A63U and G52A/C62U, were designed to prevent the T-stem from slipping by introducing an inside bolt in the T-stem. In the U51A/A63U mutant, the U50•A63 base pair became unpaired U50•U63 so that the Tb alignment of the T-stem was unfavorable and the Ta alignment dominated. Similarly, in G52A/C62U mutant the unpaired U51•U62 was unstable, favoring the Ta alignment of T-stem. Another mutant, U51G, was constructed to facilitate a T-stem slip by forming a base pair between G51 and C62, thus favoring a Tb alignment. In the U51G mutant, the T-stem slip reduced the size of the variable loop 1 nt (from 4 to 3) and enlarged the T-loop by 1 nt (from 7 to 8) relatively. To ascertain the effect of the alteration on aminoacylation of hmtRNA^{Leu}(CUN), mutants were constructed with a 3 nt variable loop or 8 nt T-loop. The Δ48 mutant had a deleted nucleotide at position 48 to test the effect of a reduced variable loop and the U48C/+G54 mutant contained 8 nt in its T-loop.

The design for each tRNA variant was confirmed by secondary structure prediction (data not shown). Enzymatic probing was further performed with the representative tRNA transcripts. Although the digestion signal at the T-loop was weak, probably due to the tertiary structure protection, the expected alignment patterns were still detectable. As presented in Figure 4A, no dose-dependent RNase T1 cleavage site at G53 was detected in either the U51A/A63U or the Δ48 mutant, which indicated that the T-stem slip was restrained by these mutations. Meanwhile in the U51G and U48C/+G54 mutants, RNase T1 cleaved at G53 and G54, respectively, which was consistent with the T-loop enlargement. Moreover, some other characteristic differences in the structures of tRNA variants were detected. For example, the nucleotides in the T-stem were cleaved by RNase V1 in the 7 nt T-loop variant (Δ48, U48C and U51A/A63U), whereas T-stem cleavages did not occur in either of the mutants with an enlarged T-loop (U51G and U48C/+G54). Moreover, G10 and G11 in the D-stems of both the U51G and U48C/+G54 mutants were cleaved by RNase T1, suggesting that the T-loop enlargements induced changes in their D-loops. These differences most likely reflect domain–domain interactions between the D- and T-loops in

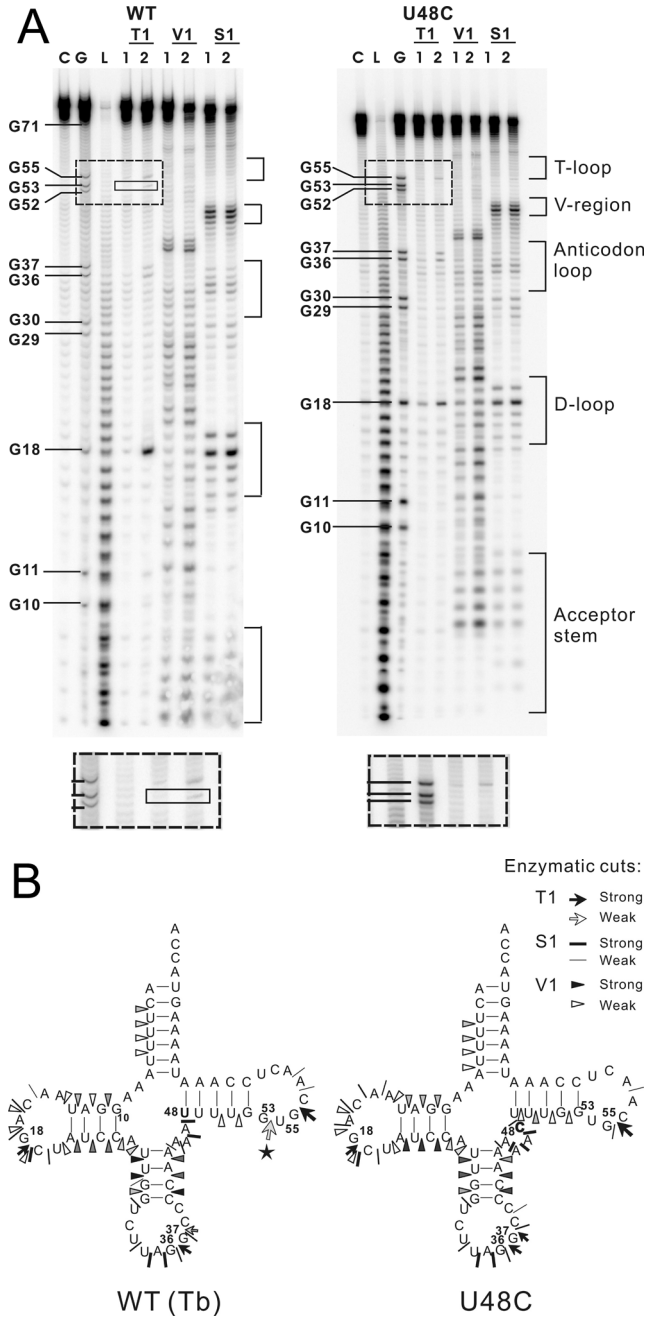

Figure 3. Comparative enzymatic probing of *in vitro* transcribed human mitochondrial tRNA^{Leu}(CUN) and the U48C mutant. (**A**) Autoradiograms of the various cleavage products of 5′-end-labeled tRNA transcripts separated on denaturing 12% polyacrylamide gels. Lane C, control incubations without probe; lane L, alkaline ladder; lane G, G ladder. The tRNA was 5′-labeled and digested with RNase T1, RNase V1 and nuclease S1. Numbers 1 and 2 refer to increasing concentrations of nuclease. The RNase T1 cleavage product specific for WT transcript was indicated in the solid-line square. The difference can be easily seen in the dashed-line squares. (**B**) Result of the enzymatic probing of WT and U48C mutant hmtRNA^{Leu}(CUN) transcripts. Intensities of cuts are proportional to the darkness of the symbols. The pentacle denotes the specific RNase T1 cleavage at G53 on WT transcript.

hmtRNA^{Leu}(CUN). The patterns of enzymatic digestion of each tRNA mutant are given in Figure 4B.

The charging efficiency of hmLeuRS for each designed tRNA variant was examined. The accepting activities of these mutants are shown in Figure 5 and the kinetic parameters are presented in Table 1. The aminoacylation of the three U48N (N = A, G, C) mutants increased similarly compared with the WT transcript. The results indicate that the increased accepting activity of the U48C mutation is due to the secondary structure rather than a specific residue substitution. The two T-stem double mutants showed greater increases (2.91-fold for U51A/A63U and 2.13-fold for G52A/C62U as compared with that for WT transcript) in charging efficiency (k_{cat}/K_M) than those of U48 mutants, suggesting that the stability of Ta alignment and instability of Tb alignment is very important for the accepting activity. The Δ48 mutant, which mimicked the shortened variable loop resulting from a T-stem slip, also presented increased plateau level (65%) and charging efficiency (1.61-fold increase relative to WT). It is possible that the shortened variable loop inhibited T-stem slip, favoring the Ta alignment. Conversely, the U51G mutation that promoted the T-stem slip, favoring the Tb alignment, dramatically decreased the charging activity of hmtRNA^{Leu}(CUN). Less than 0.5% of the U51G mutant was aminoacylated following a 40 min incubation under the experimental conditions. The U48C/+G54 mutation with the 8 nt T-loop, which mimicked the T-loop induced by a T-stem slip, also showed decreased aminoacylation. Neither of these two mutants displayed sufficient aminoacylation to determine the kinetic parameters. This result suggests that the size of the T-loop is critical for the tRNA charging activity in that charging capacity is decreased by the addition of bases into the T-loop, even when T-stem is unchanged. The data suggest that the negative effect of a T-stem slip on aminoacylation of hmtRNA^{Leu}(CUN) is due to the increased size of the T-loop induced by the slip.

DISCUSSION

Comparison of the variable loops and T-stems of *E.coli* (21), *Aquifex aeolicus* (22) and human cytoplasmic (23) tRNA^{Leu}s with those of hmtRNA^{Leu}(CUN) indicates that there are several features that determine whether a tRNA^{Leu}s structure is conducive to a T-stem slip. All 5 bp in the T-stem of *E.coli* tRNA^{Leu}(CUG) and *A.aeolicus* tRNA^{Leu}(CUC) and the 4 bp in the T-stem of *E.coli* tRNA^{Leu}(CUC) and human cytoplasmic tRNA^{Leu}(CUU) are GC pairs. This high level of GC base pairing in the T-stem stabilizes the Ta alignment and thereby inhibits a T-stem slip in the above tRNA^{Leu}s. A T-stem slip is further disabled by the inability of the base at position 48 in the variable loop to form a base pair with the base at position 65 in these tRNA^{Leu}s. Finally, the large size of the variable loops in these Ta stable tRNA^{Leu}s (12–16 nt and 2–4 bp) is a hindrance to a T-stem slip. In contrast, because only 2 of the 5 bp of the T-stem are GC pairs in hmtRNA^{Leu}(CUN), the Ta structure configuration is less stable than that in the above tRNAs. Moreover, in hmtRNA^{Leu}(CUN) U48 exactly pairs with A65 following a T-stem slip, and the variable loop is smaller containing only 4 nt and no base pair. These unique structural features of hmtRNA^{Leu} (CUN) enable a T-stem slip.

The inherently fragile structure of hmtRNA has been discussed previously (24–26). In this work, the structural fragility of hmtRNA^{Leu}(CUN) is specified as a mechanism of T-stem slip. The T-stem slip can result in a mixture of Ta and Tb

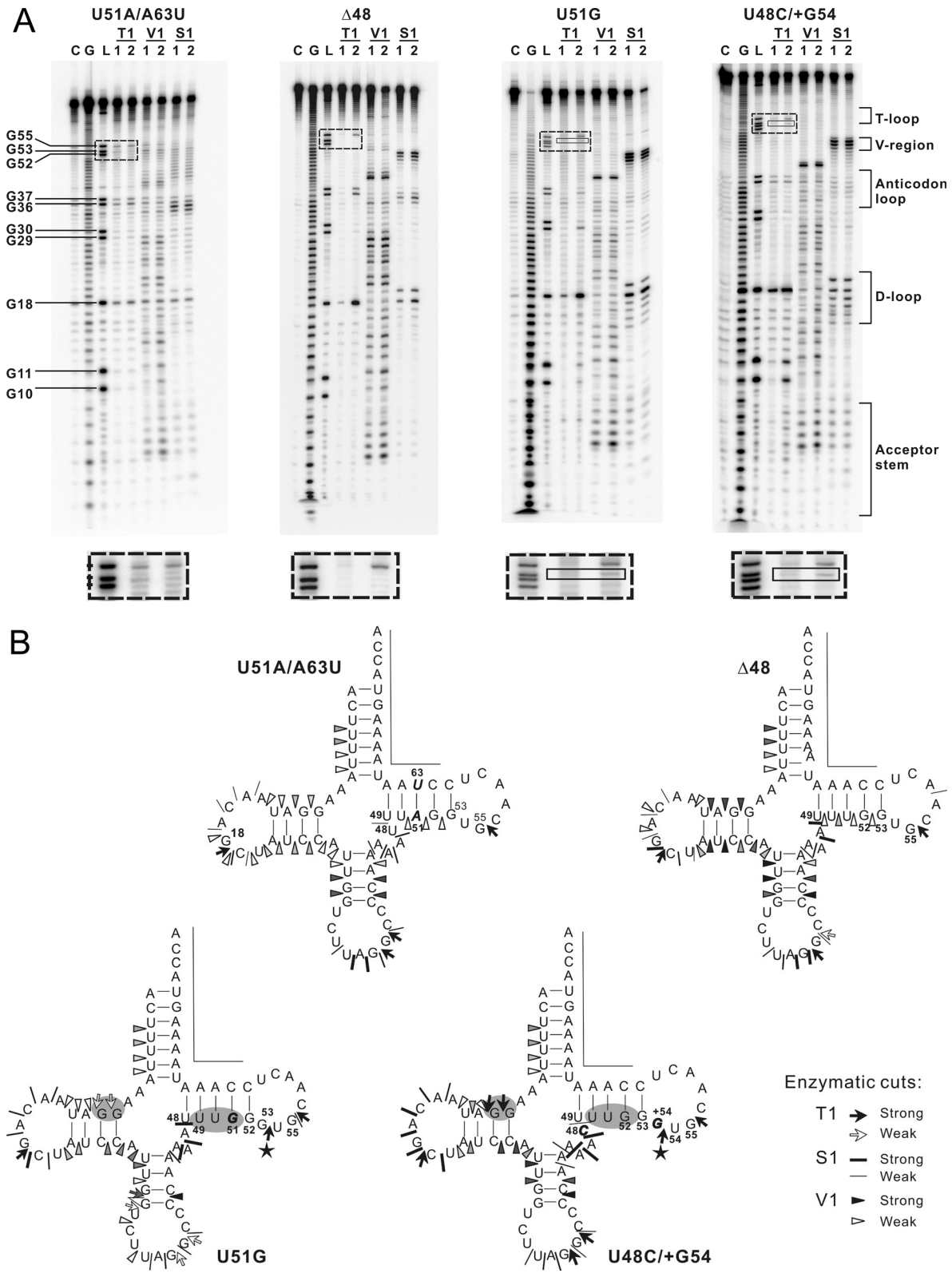

Figure 4. Enzymatic probing of the representative $tRNA^{Leu}$(CUN) variants. (**A**) Cleavage products of 5′-labeled molecules after treatment with nucleases, displayed on autoradiograms of 12% polyacrylamide gels. C stands for H_2O ladder; G for G ladder; L for alkaline ladder; T1 for RNase T1 digestion ladder; V1 for RNase V1 digestion ladder; S1 for nuclease S1 digestion ladder; numbers 1 and 2 refer to increasing concentrations of nuclease. The RNase T1 cleavage product denoted in the solid-line square indicates the enlarged T-loop. The band difference can be easily seen in the dashed-line squares. (**B**) Location of enzymatic cleavage sites on cloverleaf diagrams of the transcripts. Specifications and intensities of cuts are as indicated in the key. Nucleotides that could not be tested because of technical limitations are marked by a line. Mutated nucleotides are shown in italics. Regions with different cleavage pattern are highlighted by gray background. The pentacles denote the RNase T1 cleavage specific for the enlarged T-loop.

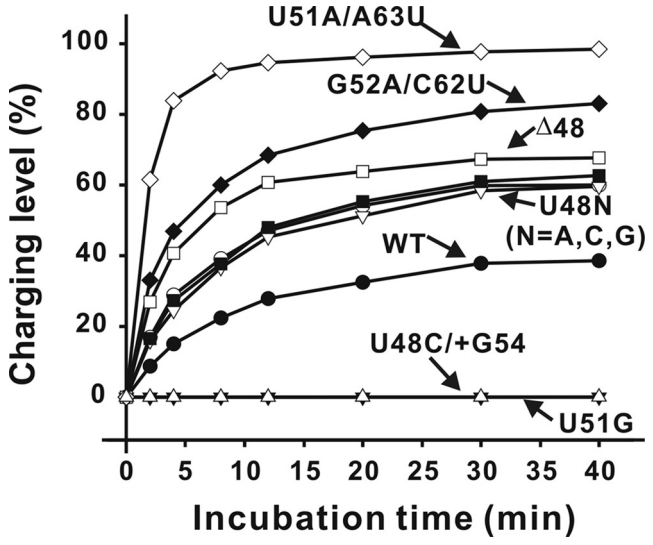

Figure 5. Effects of the designed mutations on aminoacylation capacity of hmtRNA^{Leu}(CUN). All values were the average of three experiments. The standard errors were <5%.

alignments among the WT hmtRNA^{Leu}(CUN). Mutation analysis indicates that the T-stem slip, especially the varied size of the T-loop, correlates with the charging capacity. When its T-stem presents a Ta alignment and the T-loop contains 7 nt, the tRNA can be charged. While the T-stem slips to the Tb alignment and the T-loop is enlarged to 8 nt, the accepting capacity is lost. The T-stem slip appears to function as a switch for the charging capacity of hmtRNA^{Leu}(CUN).

As the T-stem is generally not a locus for tRNA^{Leu}s recognition in systems including *E.coli*, *Haloferax volcanii*, *Saccharomyces cerevisiae* and human mitochondria (27–32), it is highly probable that the T-stem slip in hmtRNA^{Leu}(CUN) governs its charging capacity by inducing a change in tRNA tertiary structure. Enzymatic probing experiments reveal the D-stem relaxation in mutants with an enlarged T-loop (Figure 4), indicating domain–domain interactions between the D- and T-loops in hmtRNA^{Leu}(CUN). Considering the interdomain interactions found in other hmtRNAs (25,26,33), the prevalence of intramolecular communication could be expected in the tRNA possessing a fragile structure.

The generation of a functional tRNA is a complicated process with many steps, including transcription, end-processing, post-transcriptional modification, aminoacylation and participation in ribosomal protein synthesis. Previous work has shown that a tRNA molecule can assume different conformations to interact with different partners (34–36). The alternative conformations of hmtRNA^{Leu}(CUN) that result from the T-stem slip may be required for its optimal interaction with the processing enzymes or the translation apparatus in human mitochondria. It is possible that the conformations in equilibrium may change according to the requirements of the mitochondrion. Because a mitochondrion is a primitive organelle, such a minute structural change may provide an economical mechanism for functional regulation of hmtRNA. However, once the T12311C mutation was introduced into the U48C mutant, the T-stem slip 'switch' was destroyed, preventing the change from the Ta alignment to the Tb alignment and inhibiting the regulation of the charging capacity. Thus, we hypothesize that it is either the fixed charging capacity or the frozen structure of the U48C mutant that may be the cause of the related disease.

Usually, *in vitro* transcription is an efficient approach to study the contribution of an individual nucleotide to tRNA structure and function (6,8,24–26). Owing to the absence of post-transcriptional modifications, different properties between the transcripts and their native counterparts were discovered (18,27,37,38). Based on this knowledge, although the hmtRNA^{Leu}(CUN) transcript appears to fold correctly and is aminoacyable, it mimics the native tRNA mainly at an immature level. Further *in vivo* study will be helpful to elucidate the mechanism of the related diseases.

ACKNOWLEDGEMENTS

This work was funded by the Natural Science Foundation of China (Grant 30270310 and 30330180), Committee of Science and Technology in Shanghai (Grant 02DJ140567) and the 863 projects of China (Grant 2004AA235091). Funding to pay the Open Access publication charges for this article was provided by the National Science Foundation of China (Grant 30270310).

Conflict of interest statement. None declared.

REFERENCES

1. Söll,D. (1993) Transfer RNA: an RNA for all season. In Gestelandm,R.F. and Atkins,J.F. (eds), *The RNA World*. Cold Spring Harbor Laboratory Press, Cold Spring Harbor, NY, pp. 157–183.
2. Anderson,S., Bankier,A.T., Barrell,B.G., de Bruijn,M.H., Coulson,A.R., Drouin,J., Eperon,I.C., Nierlich,D.P., Roe,B.A., Sanger,F. *et al*. (1981) Sequence and organization of the human mitochondrial genome. *Nature*, **290**, 457–465.
3. Helm,M., Brule,H., Friede,D., Giegé,R., Putz,D. and Florentz,C. (2000) Search for characteristic structural features of mammalian mitochondrial tRNAs. *RNA*, **6**, 1356–1379.
4. Pulkes,T. and Hanna,M.G. (2001) Human mitochondrial DNA diseases. *Adv. Drug Deliv. Rev.*, **49**, 27–43.
5. Florentz,C. and Sissler,M. (2001) Disease-related versus polymorphic mutations in human mitochondrial tRNAs. Where is the difference? *EMBO Rep.*, **2**, 481–486.
6. Kelley,S.O., Steinberg,S.V. and Schimmel,P. (2000) Functional defects of pathogenic human mitochondrial tRNAs related to structural fragility. *Nature Struct. Biol.*, **7**, 862–865.
7. Wittenhagen,L.M. and Kelley,S.O. (2003) Impact of disease-related mitochondrial mutations on tRNA structure and function. *Trends Biochem. Sci.*, **28**, 605–611.
8. Levinger,L., Morl,M. and Florentz,C. (2004) Mitochondrial tRNA 3′ end metabolism and human disease. *Nucleic Acids Res.*, **32**, 5430–5441.
9. Nakamura,Y., Gojobori,T. and Ikemura,T. (2000) Codon usage tabulated from international DNA sequence databases: status for the year 2000. *Nucleic Acids Res.*, **28**, 292.
10. Hattori,Y., Goto,Y., Sakuta,R., Nonaka,I., Mizuna,Y. and Horai,S. (1994) Point mutations in mitochondrial tRNA genes: sequence analysis of chronic progressive external ophthalmoplegia (CPEO). *J. Neurol. Sci.*, **125**, 50–55.
11. Dirheimer,G., Keith,G., Dumas,P. and Westhof,E. (1995) Primary, secondary and tertiary structures of tRNAs. In Söll,D. and RajBhandary,U.L. (eds), *tRNA Structure, Biosynthesis and Function*. American Society for Microbiology, Washington DC, pp. 93–126.
12. Li,Y., Wang,E.D. and Wang,Y.L. (1999) A modified procedure for fast purification of T7 RNA polymerase. *Protein Expr. Purif.*, **16**, 355–358.
13. Yao,Y.N., Wang,L., Wu,X.F. and Wang,E.D. (2003) Human mitochondrial leucyl-tRNA synthetase with high activity produced from *Escherichia coli*. *Protein Expr. Purif.*, **30**, 112–116.

14. Hao,R., Yao,Y.N., Zheng,Y.G., Xu,M.G. and Wang,E.D. (2004) Reduction of mitochondrial $tRNA^{Leu}$(UUR) aminoacylation by some MELAS-associated mutations. *FEBS Lett*., **578**, 135–139.
15. Puglisi,J.D. and Tinoco,I.,Jr (1989) Absorbance melting curves of RNA. *Methods Enzymol*., **180**, 304–325.
16. Zuker,M. (2003) Mfold web server for nucleic acid folding and hybridization prediction. *Nucleic Acids Res*., **31**, 3406–3415.
17. Silberklang,M., Gillum,A.M. and RajBhandary,U.L. (1979) Use of *in vitro* 32P labeling in the sequence analysis of nonradioactive tRNAs. *Methods Enzymol*., **59**, 58–109.
18. Helm,M., Brule,H., Degoul,F., Cepanec,C., Leroux,J.P., Giegé,R. and Florentz,C. (1998) The presence of modified nucleotides is required for cloverleaf folding of a human mitochondrial tRNA. *Nucleic Acids Res*., **26**, 1636–1643.
19. Peattie,D.A. and Gilbert,W. (1980) Chemical probes for higher-order structure in RNA. *Proc. Natl Acad. Sci. USA*, **77**, 4679–4682.
20. Krol,A. and Carbon,P. (1989) A guide for probing native small nuclear RNA and ribonucleoprotein structures. *Methods Enzymol*., **180**, 212–227.
21. Li,T., Li,Y., Guo,N.N., Wang,E.D. and Wang,Y.L. (1999) Discrimination of $tRNA^{Leu}$ isoacceptors by the insertion mutant of *Escherichia coli* leucyl-tRNA synthetase. *Biochemistry*, **38**, 9084–9088.
22. Xu,M.G., Chen,J.F., Martin,F., Zhao,M.W., Eriani,G. and Wang,E.D. (2002) Leucyl-tRNA synthetase consisting of two subunits from hyperthermophilic bacteria *Aquifex aeolicus*. *J. Biol. Chem*., **277**, 41590–41596.
23. Chang,Y.N., Pirtle,I.L. and Pirtle,R.M. (1986) Nucleotide sequence and transcription of a human tRNA gene cluster with four genes. *Gene*, **48**, 165–174.
24. Sohm,B., Frugier,M., Brule,H., Olszak,K., Przykorska,A. and Florentz,C. (2003) Towards understanding human mitochondrial leucine aminoacylation identity. *J. Mol. Biol*., **328**, 995–1010.
25. Kelley,S.O., Steinberg,S.V. and Schimmel,P. (2001) Fragile T-stem in disease-associated human mitochondrial tRNA sensitizes structure to local and distant mutations. *J. Biol. Chem*., **276**, 10607–10611.
26. Roy,M.D., Wittenhagen,L.M., Vozzella,B.E. and Kelley,S.O. (2004) Interdomain communication between weak structural elements within a disease-related human tRNA. *Biochemistry*, **43**, 384–392.
27. Sohm,B., Sissler,M., Park,H., King,M.P. and Florentz,C. (2004) Recognition of human mitochondrial tRNALeu(UUR) by its cognate leucyl-tRNA synthetase. *J. Mol. Biol*., **339**, 17–29.
28. Larkin,D., Williams,A., Martinis,S. and Fox,G. (2002) Identification of essential domains for *Escherichia coli* tRNALeu aminoacylation and amino acid editing using minimalist RNA molecules. *Nucleic Acids Res*., **30**, 2103–2113.
29. Tocchini-Valentini,G., Saks,M.E. and Abelson,J. (2000) tRNA leucine identity and recognition sets. *J. Mol. Biol*., **298**, 779–793.
30. Asahara,H., Nameki,N. and Hasegawa,T. (1998) *In vitro* selection of RNAs aminoacylated by *Escherichia coli* leucyl-tRNA synthetase. *J. Mol. Biol*., **283**, 605–618.
31. Soma,A., Uchiyama,K., Sakamoto,T., Maeda,M. and Himeno,H. (1999) Unique recognition style of $tRNA^{Leu}$ by *Haloferax volcanii* leucyl-tRNA synthetase. *J. Mol. Biol*., **293**, 1029–1038.
32. Soma,A., Kumagai,R., Nishikawa,K. and Himeno,H. (1996) The anticodon loop is a major identity determinant of *Saccharomyces cerevisiae* $tRNA^{Leu}$. *J. Mol. Biol*., **263**, 707–714.
33. Watanabe,Y., Tsurui,H., Ueda,T., Furushima,R., Takamiya,S., Kita,K., Nishikawa,K. and Watanabe,K. (1994) Primary and higher order structures of nematode (*Ascaris suum*) mitochondrial tRNAs lacking either the T or D stem. *J. Biol. Chem*., **269**, 22902–22906.
34. Ishitani,R., Nureki,O., Nameki,N., Okada,N., Nishimura,S. and Yokoyama,S. (2003) Alternative tertiary structure of tRNA for recognition by a posttranscriptional modification enzyme. *Cell*, **113**, 383–394.
35. Randau,L., Schauer,S., Ambrogelly,A., Salazar,J.C., Moser,J., Sekine,S., Yokoyama,S., Söll,D. and Jahn,D. (2004) tRNA recognition by glutamyl-tRNA reductase. *J. Biol. Chem*., **279**, 34931–34937.
36. Hauenstein,S., Zhang,C.M., Hou,Y.M. and Perona,J.J. (2004) Shape-selective RNA recognition by cysteinyl-tRNA synthetase. *Nature Struct. Mol. Biol*., **11**, 1134–1141.
37. Kirino,Y., Yasukawa,T., Ohta,S., Akira,S., Ishihara,K., Watanabe,K. and Suzuki,T. (2004) Codon-specific translational defect caused by a wobble modification deficiency in mutant tRNA from a human mitochondrial disease. *Proc. Natl Acad. Sci. USA*, **101**, 15070–15075.
38. Sissler,M., Helm,M., Frugier,M., Giegé,R. and Florentz,C. (2004) Aminoacylation properties of pathology-related human mitochondrial tRNA(Lys) variants. *RNA*, **10**, 841–853.
39. Sprinzl,M., Horn,C., Brown,M., Ioudovitch,A. and Steinberg,S. (1998) Compilation of tRNA sequences and sequences of tRNA genes. *Nucleic Acids Res*., **26**, 148–153.